ACS OMEGA

http://pubs.acs.org/journal/acsodf

Review

Resonant Enhancement of Polymer–Cell Optostimulation by a Plasmonic Metasurface

Arijit Maity,[¶] Sara Perotto,[¶] Matteo Moschetta, Huang Hua, Samim Sardar, Giuseppe Maria Paternò, Jingyi Tian, Maciej Klein, Giorgio Adamo, Guglielmo Lanzani,* and Cesare Soci*

Cite This: *ACS Omega* 2022, 7, 42674–42680

Read Online

ACCESS | Metrics & More | Article Recommendations | Supporting Information

ABSTRACT: Organic semiconductors have shown great potential as efficient bioelectronic materials. Specifically, photovoltaic polymers such as the workhorse poly(thiophene) derivatives, when stimulated with visible light, can depolarize neurons and generate action potentials, an effect that has been also employed for rescuing vision in blind rats. In this context, however, the coupling of such materials with optically resonant structures to enhance those photodriven biological effects is still in its infancy. Here, we employ the optical coupling between a nanostructured metasurface and poly(3-hexylthiophene) (P3HT) to improve the bioelectronic effects occurring upon photostimulation at the abiotic–biotic interface. In particular, we designed a spectrally tuned aluminum metasurface that can resonate with P3HT, hence augmenting the effective field experienced by the polymer. In turn, this leads to an 8-fold increase in invoked inward current in cells. This enhanced activation strategy could be useful to increase the effectiveness of P3HT-based prosthetic implants for degenerative retinal disorders.

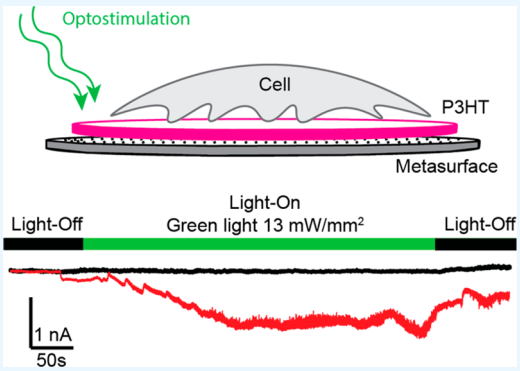

INTRODUCTION

The use of organic electronic devices in bioelectronics has seen a steep rise in the last couple of decades.[1−4] One of the most important reasons is that organic semiconductors share many common features with biological matter, such as softness (i.e., in terms of supramolecular interaction and charge transport) and mixed ionic–electronic conduction.[5] In addition, these materials exhibit superior biocompatibility, conformability, and cost-effectiveness compared to their inorganic counterparts.

Within this context, high flexibility and lack of an external power supply make organic electronic devices a promising tool to restore retinal activity.[6] For instance, certain retinal dystrophies such as macular degeneration and retinitis pigmentosa involve degeneration of the photoreceptors, which ultimately results in severe or complete loss of vision. The current proven state-of-the-art solution to these diseases relies on the use of surgical implants of prosthetic devices that work as artificial photoreceptors. These prosthetic devices, however, have several limitations. Besides being heavy, bulky, and requiring an external power supply, there are biocompatibility issues due to the use of inorganic semiconductors and metallic electrodes. Alternatively, an organic bioelectronic device consisting of poly(3-hexylthiophene-2,5-diyl) (P3HT) has been proposed.[7] Here, a layer of P3HT deposited over a poly(3,4-ethylenedioxythiophene):polystyrenesulfonate (PEDOT:PSS) layer absorbs the incoming light and interacts with the neighboring cells, inducing a bioelectric response in neurons via a stimulation mechanism that likely involves both photothermal and photocapacitive phenomena occurring at the abiotic/biotic interface. Further improvements in the device performances have been obtained using nanostructured P3HT.[8,9] Overall, the enhancement of such photodriven phenomena, which ultimately depend on the light absorption capability of the active layer, would certainly improve device functionality and enable their use under low-light illumination.

In these regards, an interesting route would be the use of plasmonic materials or optical resonators that are spectrally tuned with P3HT absorption, so that their optical coupling would lead to an enhancement of the local electromagnetic field experienced by the polymer. Recently, metallic surfaces have been used to control the rate of P3HT photodegradation,[10,11] while the use of metamaterials to achieve field enhancement has been proposed for improving the power conversion efficiency in organic solar cells.[12,13] Some recent works investigated the optical response of such devices in biological processes.[14−16] However, to the best of our knowledge, such an approach has never been employed

Received: July 29, 2022
Accepted: September 23, 2022
Published: November 16, 2022

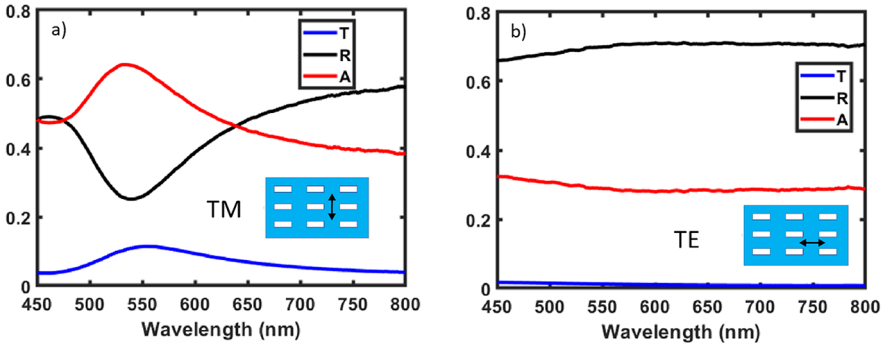

Figure 1. Spectral characteristics of the designed metasurface. Experimentally measured optical reflection (black trace), transmission (blue trace), and absorption (red trace) spectra of the nanoslit metamaterial arrays fabricated for normally incident light with polarizations perpendicular (TM, left panel) and parallel (TE, right panel) to the slits.

systematically to modulate the photodriven effects at the abiotic/biotic interface.

Here, we exploit the plasmon resonance of an aluminum metasurface that is spectrally coupled to P3HT to enhance its light absorption. After characterizing the coupling using steady-state and ultrafast spectroscopies, we applied this stimulation paradigm to photocontrol the membrane potential in human embryonic kidney cells (HEK293T). We show that, in the presence of the resonant structure, cell depolarization increases by a factor of 8, suggesting that the metamaterial plays a role in the photostimulation process.

RESULTS AND DISCUSSION

We designed a spectrally tuned metasurface (transmission and absorption peak ∼540 nm, Figure 1) to be in optical resonance with P3HT (absorption peak centered at ∼530 nm). In such a way, the metasurface is expected to concentrate the spectral field experienced by P3HT, leading to an enhancement of light absorption (field maps obtained by electromagnetic simulations reported in Figure S3). In particular, the spectrum of the metamaterial features a well-pronounced absorption line width centered at 530 nm under transverse magnetic (TM)-polarized illumination (Figure 1a), while being highly reflective under transverse electric (TE)-polarized illumination (Figure 1b).

Subsequently, we investigated the effects of the aluminum metasurface on P3HT thin film absorbance and photoluminescence. P3HT was deposited onto the Al metasurface via spin-coating, and reflectance was measured for different polarizations. The reflectance spectrum outside the nanostructured region (Figure 2, black trace) resembles the standard absorption structure of P3HT thin films. Specifically, at low energy, the π-stacked aggregates give rise to the more structured spectra, with the characteristic peaks associated with the A_{0-0} and A_{0-1} transitions.[17] In the amorphous phase,[18] the broadening of the intrachain absorption gives rise to a featureless band at higher energies. It is worth noticing that this latter band is enhanced with respect to the P3HT film on glass, due to the aluminum−polymer interaction.

In the presence of the metasurface, we observe an overall reduction of the reflectance signal, corresponding to greater absorption of the polymer film, together with an increase in the spectral contribution in the amorphous region. We attribute the overall broadening of the absorbance spectra and the different vibronic structures to the morphological organization of the polymer chains when interfaced with the nanostructured

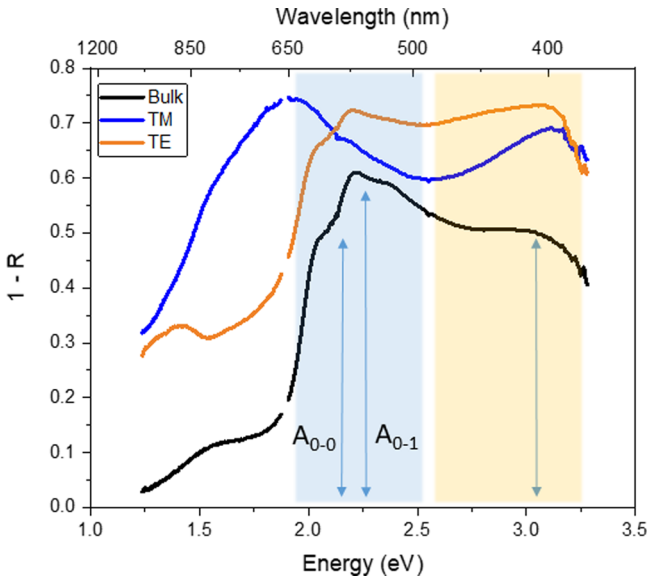

Figure 2. Spectral response of the P3HT thin film (∼30 nm) spin-coated on the metasurfaces. Experimentally measured optical reflection for normally incident light on the unpatterned aluminum (black trace) and on the nanoslit metamaterial with TE-polarized (orange trace) and TM-polarized (blue trace) light.

region.[19] Furthermore, the optical response is different for TE- and TM-polarized incident light. In particular, TE polarization induces an increased contribution of the A_{0-1} transition at 2.3 eV, in accordance with the metasurface design. Conversely, the polarization orthogonal to the nanoslits (TM) is more sensitive to the alignment of the polymer chains, resulting in red-shifted and relatively broad line width.

We then studied the metasurface−polymer interface using time-resolved spectroscopy, with the aim of elucidating the effect of field enhancement brought about by the metamaterial on the P3HT deactivation pathways. Indeed, the study of time-resolved fluorescence provides significant information on the decay rates and relaxation dynamics which are particularly sensitive to the polymer organization and its environment. We carried out experiments with two different P3HT film thicknesses, namely, 10 and 150 nm. Our initial hypothesis was that thinner films would feel the electromagnetic enhancement more effectively than thicker ones, owing to the proximity effect and the larger weight of polymer crystalline domains and planar morphology.

https://doi.org/10.1021/acsomega.2c04812
ACS Omega 2022, 7, 42674−42680

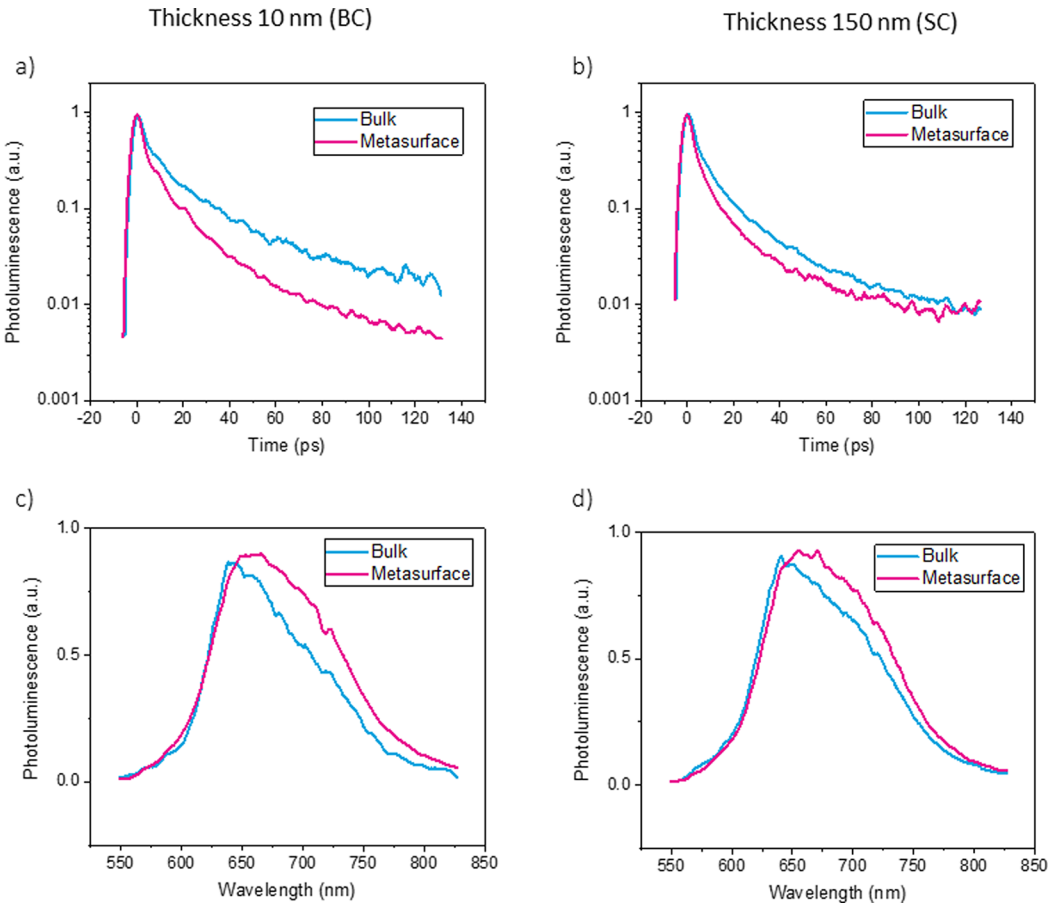

Figure 3. Time-resolved photoluminescence. PL dynamics for 10 nm (a) and 150 nm (b) thick P3HT film. PL emission spectra of 10 nm (c) and 150 nm (d) thick P3HT film. Excitation wavelength 520 nm, P = 15 μW.

Both temporal and spectral features of the photoluminescence are reported in Figure 3. For both film thicknesses, the PL time decay is faster in correspondence to the metasurface patterned area: 30% variation in 10 nm film (22.2 ± 0.4, 15.4 ± 0.3 ps on the flat and nanopatterned surface, respectively) and 20% in 150 nm film (24.56 ± 1.8, 19.9 ± 1.3 ps on the flat and nanopatterned surface, respectively). We attribute this change to the presence of an additional nonradiative deactivation channel located at the nanopatterned region, which accelerates the photoluminescence decay. Indeed, the interaction between the metasurface and the P3HT film is more evident in the thinner film, whereas the thicker one shows a behavior more similar to that in the bulk.[20] It is worth noticing that the emission spectra reported in Figure 3c,d displays a more pronounced shoulder at lower energies, due to the emission of planarized polymer chains, in the metasurface region. This can be attributed to the increase of interchain interactions due to planarization of the polymer moieties.

Finally, we proceeded to test the effect of the metasurfaces on the cell photostimulation ability of P3HT, using whole-cell patch-clamp experiments (Figure 4). It has been previously reported that long-lasting photostimulation of cells plated onto a P3HT film prompts an inward current associated with a strong membrane voltage depolarization.[21] However, the mechanism at the base of this phenomenon has not been fully clarified. Since it has been hypothesized that P3HT can form reactive oxygen species upon light stimulation, which may result in a local change of pH near its surface, we overexpressed an acid-sensing ion channel (*ASIC2a*) in HEK293T cells. These ion channels are known to be expressed in neurons and are activated by H^+.[22] Therefore, they act as a reporter of local pH change. Cells were seeded on poly-L-lysine-coated glass coverslips (with or without a coated P3HT thin film of ∼20 nm). No current was induced upon application of green light in cells seeded on bare glass in the absence of P3HT (Figure S1a). However, in the presence of the P3HT layer, both *ASIC2a*-transfected and control cells (without *ASIC2a* transfection) showed similar current induction under illumination with green light (Figure S1b−d). Upon changing the external solution to pH 4.0, strong current induction was observed which was due to the *ASIC2a* activation (Figure S1a,c). These data indicate that local pH does not change at the surface of P3HT upon photostimulation. The induced inward current in the HEK293T cells presented above could be generated either due to the heating effect at the surface of P3HT upon photostimulation or due to the activation of one or more intrinsic ion channels.

It had been shown that photostimulation of a P3HT:PCBM blend promoted membrane depolarization of primary rat hippocampal neurons grown on top of the former, eventually leading to the generation of action potential.[23] Furthermore, it was shown that a polymeric P3HT:PCBM blend induced membrane depolarization in primary astrocytes upon photostimulation and selectively activated the chloride CIC-2 channels.[21] We therefore set out to investigate which ion channels were activated in HEK293T cells upon light stimulation. Replacing the $CaCl_2$ in the solution with ethylene glycol bis(β-aminoethyl ether)-*N*,*N*,*N*′,*N*′-tetraacetic acid

https://doi.org/10.1021/acsomega.2c04812
ACS Omega 2022, 7, 42674−42680

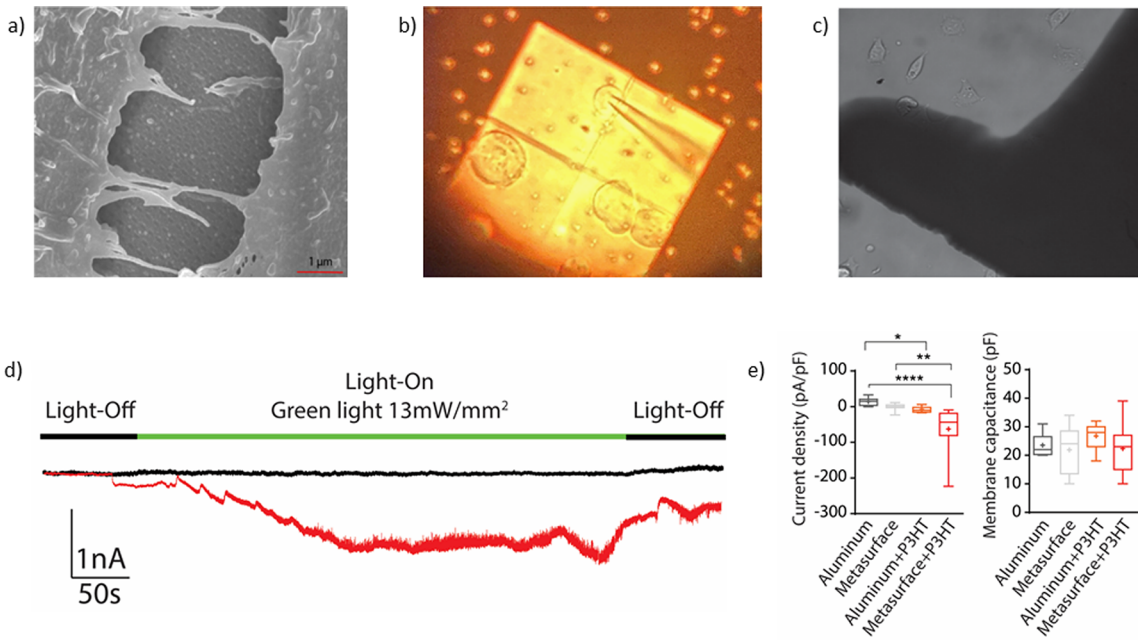

Figure 4. Visualization of cells grown on the metasurface. (a) High-resolution scanning electron microscopy image recorded in secondary electron imaging mode with 5 kV acceleration voltage and 17000× magnification. (b) Bright-field image of the patch-clamp measurement. (c) Confocal microscopy image on the metamaterial/on the control pad. Effect of photostimulation on HEK293T cells seeded on different substrates. (d) Representative traces of the photocurrents generated by HEK293T cells seeded on coverslips containing metasurface (black) or metasurface + P3HT (red) during light stimulation. (e) Histograms showing the maximal current density after 4 min of light stimulation (right) and cell membrane capacitance (left). The mean current of the baseline was subtracted from the peak current (pA) during the photostimulation and normalized against the cell capacitance (pF); $N = 8$, 12, 8, and 11 for cells plated on aluminum, metasurface, aluminum + P3HT, and metasurface + P3HT, respectively; $*p < 0.05$; $**p < 0.01$, $****p < 0.0001$; Kruskal–Wallis test followed by Dunn's correction. Data are presented as box plots with whiskers representing the minimum and the maximum values.

(EGTA) did not affect the current significantly (Figure S2, right panel); on the other hand, replacing NaCl with choline chloride diminished the inward current drastically (Figure S2, left panel). These findings suggest that Na^+ rather than Ca^{2+} ion channels are involved in the photostimulation with P3HT. Nonetheless, the addition of choline chloride did not completely eliminate the occurrence of light-evoked inward current. Hence, the elicitation of this current is determined by the superposition of multiple phenomena, including Na^+ channel activation. We proceeded by testing the effect of metasurfaces on the light-evoked inward current of HEK293T cells plated on the top of a 30 nm thick P3HT film (Figure 4a). The HEK293T cells were stimulated with the same power density used in previous experiments.[21] We observed that green light stimulation (13 mW/mm^2) elicits a consistent inward current (−62 ± 20.11 pA/pF) in cells plated onto the P3HT-coated metasurface. In addition, cells plated onto the uncoated metasurface displayed no significant light-evoked inward current (Figure 4d,e). To verify the contribution of the metasurface in this process, we photostimulated cells plated on the top of either P3HT-uncoated or -coated aluminum. In particular, P3HT-coated aluminum was able to generate a light-dependent inward current in HEK293T cells; however, the peak current was significantly lower compared to that of one of the cells plated onto the P3HT-coated metasurface (−62 ± 20.11 vs −8 ± 2.88 pA/pF). In addition, it is clear that different surfaces do not alter cell passive membrane properties, as cell membrane capacitance remains unaltered under dark conditions (Figure 4e). The presence of conductance mediated by Na^+ channels in non-excitable cells is still debated even if few works reported the expression of TTX-sensitive Na^+ currents in HEK293T cells.[24] The mechanisms of activation of Na^+ conductance in HEK293T cells is still unknown, but we can hypothesize that strong membrane depolarization can activate these channels. Membrane depolarization can occur after cytoskeletal disruption upon photolysis. However, we did not observe any membrane swelling/blebbing or any other morphological changes that could confirm this hypothesis. The depolarization of the membrane potential was previously reported by Benfenati et al. and Martino et al.[21,25] In those cases, the authors suggested that the depolarization might be due to both the accumulation of positive charges at the polymer surface and a photothermal phenomenon.[21,23] Martino and collaborators demonstrated that during light stimulation temperature increases locally at the level of the P3HT/HEK293T cells interface. An illumination power density of 15 mW/mm^2 was shown to be able to elicit an increase of temperature of about 1 °C even at low-lasting light stimulation (20–200 ms) associated with a transient membrane depolarization.[25] Lower power densities (∼1 mW/mm^2) may not cause a significant increase in the local temperature; however, a prolonged light exposure (4–5 min) even at these lower power densities should be sufficient to elicit a thermal-dependent depolarization. It is therefore reasonable to hypothesize in our experimental model that photostimulation induces a local temperature increase sufficient to elicit a sustained depolarization and trigger Na^+ channel activation.

CONCLUSIONS

In this work, we presented an approach to boost the photodriven biological effects brought about by P3HT

https://doi.org/10.1021/acsomega.2c04812
ACS Omega 2022, 7, 42674−42680

illumination. In particular, we employed plasmonic resonant structures made of aluminum metasurface to enhance the local electromagnetic field at the interface with P3HT. We found that, besides increasing the overall P3HT film absorption, the nanostructured surface affects the polythiophene chains' organization in the films, affecting the crystallinity of film domains and leading to a preferential direction of chain planarization. This different morphology has been inferred by reflectance measurements and time-gated PL spectra. Furthermore, the difference in the excited-state dynamics between the P3HT−Al bulk region and the P3HT−Al metasurface region highlights the role of the resonant metasurface in the relaxation processes. Indeed, the fastening of the decay at the metasurface suggests that another nonradiative path becomes available. Finally, the metasurface has been proven to play an active role in the photostimulation process, inducing cells' depolarization increase by nearly 1 order of magnitude. Thanks to the flexibility of metasurface design and the complexity of induced interactions, we believe that this work may pave the way for the use of resonant nanostructures in the study of the mechanisms taking place at the biotic/abiotic interface.

METHODS

Preparation of P3HT Films. Regioregular P3HT (rr-P3HT, M_w 50000−70000) was purchased from Sigma-Aldrich Ltd. Aluminum substrates were cleaned with acetone and isopropyl alcohol (IPA) followed by thermal treatment at 60 °C for 5 min. 1,2-Chlorobenzene solution of rr-P3HT (5 and 10 g L^{-1}) was spin-coated on the Al substrates. Spinning parameters were set (step 1: 800 rpm, angular acceleration 1500 rad s^{-2}, duration 3 s; step 2: 2000 rpm, angular acceleration 1500 rad s^{-2}, duration 60 s) to obtain films of ∼30 and ∼150 nm thickness for each polymer solution concentration. 1,2-Chlorobenzene solution of rr-P3HT (10 g L^{-1}) was deposited using a wire bar coater (TQC Sheen Automatic Film Applicator AB4400, equipped with a homemade system to control the gap between the substrate and the wire bar) to obtain the thinnest P3HT film of ∼10 nm.

Fabrication of the Metasurfaces. We selected a basic metamaterial design, a periodic array of nanoscale slits carved onto a continuous metallic film, which supports dipolar resonances in the visible spectral range whose wavelength is determined by the slit length. The metamaterials are fabricated by focused ion beam milling of a ∼50 nm thin aluminum layer and evaporated over a glass substrate. The arrays feature a slit length L of 110 nm, a slit width $W \approx 35$ nm, and a square lattice periodicity of $P = 2L$.

Cell Culture Maintenance. In vitro electrophysiological experiments were performed using the immortalized cell line HEK293T (human embryonic kidney), purchased from ATCC. HEK293T cells were cultured in T-25 cell culture flasks containing Dulbecco's modified Eagle medium high glucose (DMEM-HG) culture medium, supplemented with 10% heat-inactivated fetal bovine serum and 1% GlutaMAX (0.5 mM, Invitrogen). Culture flasks were maintained in a humidified incubator at 37 °C with 5% CO_2. When at confluence, cells were enzymatically detached from the flasks with a 1× trypsin-EDTA solution, plated on sterilized substrates, and left to grow for 48 h before the recordings. Prior to cell plating, a layer of fibronectin (2 μg mL^{-1} in phosphate-buffered saline solution) was deposited on the sample surface and incubated for 1 h at 37 °C to promote cellular adhesion.

Scanning Electron Microscopy. The cells were fixed on the metasurface by applying 2% paraformaldehyde solution for 20 min. The fixed cells were then dehydrated by applying an increasing concentration of absolute ethanol (50, 70, 90 and 100%) for about 5−15 min. After this, the cells underwent a chemical dehydration protocol using bis(trimethylsilyl)amine (HMDS) overnight. A 10 nm Pt coating was applied to make the cells conductive. Scanning electron microscopy imaging was carried out using JEOL-JSM-7600F microscope in secondary electron imaging mode with an operating voltage of 5.0 kV and a magnification of 17000×.

Electrophysiology. Standard patch-clamp recordings were performed with an Axopatch 700 B (Axon Instruments) coupled with an Olympus BX53 biological microscope. HEK293T cells were measured in whole-cell configuration with freshly pulled glass pipettes (4−7 MΩ), filled with the following intracellular solution [mM]: 12 KCl, 125 K-gluconate, 1 $MgCl_2$, 0.1 $CaCl_2$, 10 EGTA, 10 HEPES, and 10 ATP-Na_2. The extracellular solution contained [mM] 135 NaCl, 5.4 KCl, 5 HEPES, 10 glucose, 1.8 $CaCl_2$, and 1 $MgCl_2$. Acquisitions were performed with pClamp-10 software (Axon Instruments). Membrane currents were low-pass-filtered at 2 kHz and digitized with a sampling rate of 10 kHz (Digidata 1550B, Molecular Devices). A green light-emitting diode coupled to the fluorescence port of the microscope and characterized by a maximum emission wavelength of 545 nm provided the excitation light source. The illuminated spot on the sample had an area of 0.23 mm^2 and a photoexcitation density of 13 mW/mm^2, as measured at the output of the microscope objective. Data were analyzed with GraphPad Prism 6 software.

Reflectance Measurements. Reflectance measurements were done using a halogen lamp as a white light source (halogen/deuterium fiber light source), and the beam was focused on the samples by a 40× objective and recollected by the same optics. The collected signal was acquired by a CMOS spectrometer (AvaSpec).

Time-Resolved Photoluminescence Measurements. Time-resolved photoluminescence measurements were carried out using a tunable femtosecond Ti:sapphire laser source (Chameleon Ultra II, Coherent, U.S.A.) operating at an 80 MHz repetition rate and a width of ∼150 fs. The excitation of the samples with a wavelength of 520 nm was obtained by second harmonic generation. The laser source was tuned to the wavelength of 1040 nm, and the beam was focused onto a 1 mm thick beta barium borate nonlinear crystal for the generation of second harmonic pulses at 520 nm. The emission signals were collected using a 550 nm long-pass filter and analyzed by a spectrograph (Princeton Instruments Acton SP2300) coupled to a streak camera (Hamamatsu C5680, Japan) equipped with a synchroscan voltage sweep module. Within these experiments, fluorescence intensity was obtained as a function of both wavelength and time with spectral and temporal resolutions of ∼1 nm and ∼3 ps, respectively.

ASSOCIATED CONTENT

Supporting Information

The Supporting Information is available free of charge at https://pubs.acs.org/doi/10.1021/acsomega.2c04812.

Figures S1 and S2 and Figure S3, which show additional data from patch-clamp experiments and electromagnetic simulations, respectively (PDF)

https://doi.org/10.1021/acsomega.2c04812
ACS Omega 2022, 7, 42674−42680

AUTHOR INFORMATION

Corresponding Authors

Guglielmo Lanzani − *Center for Nano Science and Technology, Istituto Italiano di Tecnologia, 20133 Milan, Italy; Department of Physics, Politecnico di Milano and Center for Nano Science and Technology, Istituto Italiano di Tecnologia, 20133 Milan, Italy;* orcid.org/0000-0002-2442-4495; Phone: (+39) 02 2399 9872; Email: guglielmo.lanzani@iit.it

Cesare Soci − *Centre for Disruptive Photonic Technologies, TPI and Division of Physics and Applied Physics, School of Physical and Mathematical Sciences, Nanyang Technological University, 637371, Singapore;* orcid.org/0000-0002-0149-9128; Phone: (+65) 6514 1045; Email: CSOCI@ntu.edu.sg

Authors

Arijit Maity − *Centre for Disruptive Photonic Technologies, TPI and Division of Physics and Applied Physics, School of Physical and Mathematical Sciences, Nanyang Technological University, 637371, Singapore;* Present Address: Institut de Biologie Structurale, CNRS, Université Grenoble Alpes, CEA, Grenoble 38044, France; orcid.org/0000-0002-2399-6600

Sara Perotto − *Center for Nano Science and Technology, Istituto Italiano di Tecnologia, 20133 Milan, Italy*

Matteo Moschetta − *Center for Nano Science and Technology, Istituto Italiano di Tecnologia, 20133 Milan, Italy*

Huang Hua − *Department of Physiology, Yong Loo Lin School of Medicine, National University of Singapore, 117456, Singapore*

Samim Sardar − *Center for Nano Science and Technology, Istituto Italiano di Tecnologia, 20133 Milan, Italy;* orcid.org/0000-0003-1783-6974

Giuseppe Maria Paternò − *Center for Nano Science and Technology, Istituto Italiano di Tecnologia, 20133 Milan, Italy; Department of Physics, Politecnico di Milano and Center for Nano Science and Technology, Istituto Italiano di Tecnologia, 20133 Milan, Italy;* orcid.org/0000-0003-2349-566X

Jingyi Tian − *Centre for Disruptive Photonic Technologies, TPI and Division of Physics and Applied Physics, School of Physical and Mathematical Sciences, Nanyang Technological University, 637371, Singapore*

Maciej Klein − *Centre for Disruptive Photonic Technologies, TPI and Division of Physics and Applied Physics, School of Physical and Mathematical Sciences, Nanyang Technological University, 637371, Singapore;* orcid.org/0000-0002-3146-4372

Giorgio Adamo − *Centre for Disruptive Photonic Technologies, TPI and Division of Physics and Applied Physics, School of Physical and Mathematical Sciences, Nanyang Technological University, 637371, Singapore;* orcid.org/0000-0003-1974-3368

Complete contact information is available at: https://pubs.acs.org/10.1021/acsomega.2c04812

Author Contributions

¶A.M. and S.P. contributed equally to this work.

Notes

The authors declare no competing financial interest.

ACKNOWLEDGMENTS

This work was supported by the Singapore Ministry of Education Academic Research Fund Tier 1 (2018-T1-002-040). We would like to thank Prof. Anh Tuân Phan and Dr. Le Tuan Anh Nguyen for the useful discussions regarding the project and for facilitating the use of the cell culture facility at the Biophysics Laboratory of NTU School of Physical and Mathematical Sciences.

REFERENCES

(1) Simon, D. T.; Gabrielsson, E. O.; Tybrandt, K.; Berggren, M. Organic Bioelectronics: Bridging the Signaling Gap between Biology and Technology. *Chem. Rev.* **2016**, *116* (21), 13009−13041.

(2) Bondelli, G.; Sardar, S.; Chiaravalli, G.; Vurro, V.; Paternò, G. M.; Lanzani, G.; D'Andrea, C. Shedding Light on Thermally Induced Optocapacitance at the Organic Biointerface. *J. Phys. Chem. B* **2021**, *125* (38), 10748−10758.

(3) Vurro, V.; Scaccabarozzi, A. D.; Lodola, F.; Storti, F.; Marangi, F.; Ross, A. M.; Paternò, G. M.; Scotognella, F.; Criante, L.; Caironi, M.; et al. A Polymer Blend Substrate for Skeletal Muscle Cells Alignment and Photostimulation. *Adv. Photonics Res.* **2021**, *2* (2), 2000103.

(4) Berggren, M.; Glowacki, E. D.; Simon, D. T.; Stavrinidou, E.; Tybrandt, K. In Vivo Organic Bioelectronics for Neuromodulation. *Chem. Rev.* **2022**, *122* (4), 4826−4846.

(5) Lanzani, G. Light touch. *Nat. Nanotechnol.* **2018**, *13* (3), 181−182.

(6) Manfredi, G.; Colombo, E.; Barsotti, J.; Benfenati, F.; Lanzani, G. Photochemistry of Organic Retinal Prostheses. *Annu. Rev. Phys. Chem.* **2019**, *70*, 99−121.

(7) Maya-Vetencourt, J. F.; Ghezzi, D.; Antognazza, M. R.; Colombo, E.; Mete, M.; Feyen, P.; Desii, A.; Buschiazzo, A.; Di Paolo, M.; Di Marco, S.; et al. A fully organic retinal prosthesis restores vision in a rat model of degenerative blindness. *Nat. Mater.* **2017**, *16* (6), 681−689.

(8) Maya-Vetencourt, J. F.; Manfredi, G.; Mete, M.; Colombo, E.; Bramini, M.; Di Marco, S.; Shmal, D.; Mantero, G.; Dipalo, M.; Rocchi, A.; et al. Subretinally injected semiconducting polymer nanoparticles rescue vision in a rat model of retinal dystrophy. *Nat. Nanotechnol.* **2020**, *15* (8), 698−708.

(9) Francia, S.; Shmal, D.; Di Marco, S.; Chiaravalli, G.; Maya-Vetencourt, J. F.; Mantero, G.; Michetti, C.; Cupini, S.; Manfredi, G.; DiFrancesco, M. L.; et al. Light-induced charge generation in polymeric nanoparticles restores vision in advanced-stage retinitis pigmentosa rats. *Nat. Commun.* **2022**, *13* (1), 3677.

(10) Peters, V. N.; Tumkur, T. U.; Zhu, G.; Noginov, M. A. Control of a chemical reaction (photodegradation of the p3ht polymer) with nonlocal dielectric environments. *Sci. Rep.* **2015**, *5*, 14620.

(11) Peters, V. N.; Alexander, R.; Peters, D. A.; Noginov, M. A. Study of the effect of excited state concentration on photodegradation of the p3ht polymer. *Sci. Rep.* **2016**, *6*, 33238.

(12) Wang, Z.; Zhao, J.; Frank, B.; Ran, Q.; Adamo, G.; Giessen, H.; Soci, C. Plasmon−Polaron Coupling in Conjugated Polymer on Infrared Nanoantennas. *Nano Lett.* **2015**, *15* (8), 5382−5387.

(13) Abdulkarim, Y. I.; Deng, L.; Muhammad, F. F.; He, L. Enhanced light absorption in the organic thin films by coating cross-shaped metamaterial resonators onto the active layers. *Results Phys.* **2019**, *13*, 102338.

(14) Caprettini, V.; Huang, J. A.; Moia, F.; Jacassi, A.; Gonano, C. A.; Maccaferri, N.; Capozza, R.; Dipalo, M.; De Angelis, F. Enhanced Raman Investigation of Cell Membrane and Intracellular Compounds by 3D Plasmonic Nanoelectrode Arrays. *Adv. Sci. (Weinh)* **2018**, *5* (12), 1800560.

(15) Huang, J. A.; Caprettini, V.; Zhao, Y.; Melle, G.; Maccaferri, N.; Deleye, L.; Zambrana-Puyalto, X.; Ardini, M.; Tantussi, F.; Dipalo, M.; et al. On-Demand Intracellular Delivery of Single Particles in Single Cells by 3D Hollow Nanoelectrodes. *Nano Lett.* **2019**, *19* (2), 722−731.

(16) Khan, M. E.; Mohammad, A.; Cho, M. H. Nanoparticles Based Surface Plasmon Enhanced Photocatalysis. In *Green Photocatalysts*; Naushad, M., Rajendran, S., Lichtfouse, E., Eds.; Springer International Publishing, 2020; pp 133−143.
(17) Clark, J.; Silva, C.; Friend, R. H.; Spano, F. C. Role of Intermolecular Coupling in the Photophysics of Disordered Organic Semiconductors: Aggregate Emission in Regioregular Polythiophene. *Phys. Rev. Lett.* **2007**, *98* (20), 206406.
(18) Brown, P. J.; Thomas, D. S.; Köhler, A.; Wilson, J. S.; Kim, J.-S.; Ramsdale, C. M.; Sirringhaus, H.; Friend, R. H. Effect of interchain interactions on the absorption and emission of poly(3-hexylthiophene). *Phys. Rev. B* **2003**, *67* (6), 064203.
(19) Spano, F. C.; Silva, C. H- and J-aggregate behavior in polymeric semiconductors. *Annu. Rev. Phys. Chem.* **2014**, *65*, 477−500.
(20) Nádaždy, V.; Gmucová, K.; Nádaždy, P.; Siffalovic, P.; Vegso, K.; Jergel, M.; Schauer, F.; Majkova, E. Thickness Effect on Structural Defect-Related Density of States and Crystallinity in P3HT Thin Films on ITO Substrates. *J. Phys. Chem. C* **2018**, *122* (11), 5881−5887.
(21) Benfenati, V.; Martino, N.; Antognazza, M. R.; Pistone, A.; Toffanin, S.; Ferroni, S.; Lanzani, G.; Muccini, M. Photostimulation of Whole-Cell Conductance in Primary Rat Neocortical Astrocytes Mediated by Organic Semiconducting Thin Films. *Adv. Healthcare Mater.* **2014**, *3* (3), 392−399.
(22) Giblin, J. P.; Comes, N.; Strauss, O.; Gasull, X. Ion Channels in the Eye: Involvement in Ocular Pathologies. *Adv. Protein Chem. Struct. Biol.* **2016**, *104*, 157−231.
(23) Ghezzi, D.; Antognazza, M. R.; Dal Maschio, M.; Lanzarini, E.; Benfenati, F.; Lanzani, G. A hybrid bioorganic interface for neuronal photoactivation. *Nat. Commun.* **2011**, *2* (1), 166.
(24) He, B.; Soderlund, D. M. Human embryonic kidney (HEK293) cells express endogenous voltage-gated sodium currents and Na v 1.7 sodium channels. *Neurosci. Lett.* **2010**, *469* (2), 268−272.
(25) Martino, N.; Feyen, P.; Porro, M.; Bossio, C.; Zucchetti, E.; Ghezzi, D.; Benfenati, F.; Lanzani, G.; Antognazza, M. R. Photothermal cellular stimulation in functional bio-polymer interfaces. *Sci. Rep.* **2015**, *5* (1), 8911.

https://doi.org/10.1021/acsomega.2c04812
ACS Omega 2022, 7, 42674−42680